Kerr microscopy on a ferrimagnetic garnet

Report written by Jelle Dionot
Practical done with Marcel Brändlein under the supervision of Catherine Gourdon

Université Pierre et Marie Curie
Institut des Nanosciences de Paris

Nanomat Master Program – Group 2
Thursday, December 15th 2011

Contents

Introduction **1**

1 Theoretical background **1**
1.1 Magnetism 1
1.2 Magnetic domains 2
1.3 Total energy 2
1.4 Faraday effect 3

2 Experimental aspects **4**
2.1 Kerr microscope set-up 4
2.2 Calibration 6

3 Results and discussion **7**
3.1 Faraday rotation 7
3.2 Period of magnetic domains 8
3.3 Hysteresis cycle 10

Conclusion **11**

Introduction

Magnetic properties at a macroscopic scale have always been one of the biggest concerns of human kind to understand and explain the behaviour of various natural compounds and have been used for centuries namely with their direct application using the magnetic field of the Earth for orientation purposes. More recently, the discovery of the giant magnetoresistance (GMR) in 1988, which awarded physicists A. Fert and P. Grünberg in 2007, lead to a revolution of data storage. Since then, the interest for magnetic materials kept increasing, either to understand the already existing materials or rather to create new ones for future applications. Among the interesting phenomena that occur in magnetic materials, the arrangement and alignment of matter at the atomic scale under the influence of an external magnetic field namely in domains, are mostly studied. Magneto-optic interactions are investigated through various microscopy techniques namely Kerr microscopy. After presenting basic principles of magnetism and the so-called magnetic domains, we present in this report the use of Kerr microscopy for the study of the domains, based on the study of a ferromagnetic garnet.

1 Theoretical background

1.1 Magnetism

First of all let's present the existing types of magnetic materials. A material can be generally either diamagnetic, paramagnetic or ferromagnetic. Diamagnetism refers to materials where the constitutive atoms exhibit no permanent magnetic moment. Furthermore, an external magnetic field applied on such materials leads to magnetization opposite to the applied field, causing a repulsive effect. This effect extinguishes when the external field is turned off. A paramagnetic material, on the contrary, shows randomly oriented magnetic moments which can align with an external magnetic field in an attractive way. Both strengths involved for these two types of magnetism are rather weak and an external field is required for such effects to be induced. However, ferromagnetic materials exhibits a spontaneous magnetization thanks to the coupling that occurs under a critical temperature called the Curie temperature T_c between the intrinsic magnetic moments which align on favoured directions. A ferromagnet is a sample with a finite spatial extension and the spontaneous magnetization generates a so-called *stray field*, which opposes to the intrinsic magnetization in order to lower it. This leads to *shape anisotropy*, where locally the magnetic moments are aligned along other directions than the easy axes, thus differing from the macroscopic magnetization, ultimately leading to magnetic domains in large ferromagnets below T_c. Physically, these magnetic domains allow the sample to lower its total energy by arranging the magnetic moments in order to reduce the overall magnetization.

The domains can be changed with an external magnetic field whose strength, if it is high enough, can orientate all the magnetic moments in one direction and therefore cancel the domains. A *saturation* can hence be reached, where the material magnetization can be preserved even though the external field is suddenly turned off: the system is magnetized. An hysteresis behaviour can be observed when applying an opposite external field, when the firstly induced magnetization has to be cancelled before an opposite magnetization and saturation can be reached.

Other magnetic properties arise, namely antiferromagnetism, where the magnetic mo-

ments are distributed in opposite directions forming an almost zero magnetization with no domains, and ferrimagnetism, characterized by various magnetic moment amplitudes according to the orientations, leading to weakened ferromagnetic behaviours.

1.2 Magnetic domains

As we mentioned it in the previous section, a magnetic material in a ferro or antiferromagnetic phase, that is to say below its critical temperature, displays domains that is to say local arrangements of thousands of atoms with magnetic moment oriented in a precise direction. However, the domains shows frontiers where the local magnetization does not change abruptly but rather progressively, within the so-called domain walls. They correspond to the region of the material where the magnetic moments change progressively their directions, thus forming the domains of various orientations. These interface are described either as Bloch walls or Néel walls. The former show variation of magnetic moments parallel to the interface of two domains, whereas the latter ones correspond to change of magnetization through the plane of the interface. The domain walls are the physical consequence of a competition between the long-range magnetic exchange among the magnetic moments and the shape anisotropy that increases the interface energy and originates from the various orientations of magnetic moments along directions distinct to the easy axes of the material. This competition usually leads to periodical patterns of regions with distinct magnetization.

One considers a finite material of thickness d with an easy axis along the z-direction, a uniaxial magnetization and domains walls more or less parallel to each other in the y-direction. On the one hand, the energy of magnetic anisotropy is noted $K_u \cos^2(\theta)$, with K_u the uniaxial *anisotropy constant* and θ the angle between the magnetic moment of a domain and the easy axis of the material. On the other hand, the magnetic exchange reads:

$$A \left(\nabla \cdot \mathbf{M}\right)^2 \propto A \left(\frac{\partial \theta}{\partial y}\right)^2 \tag{1}$$

where A is the exchange constant and $\mathbf{M}$ is the magnetization. Integrating this expression over the y-direction gives the energy per length unit. The minimization of this energy provides a further expression for the angle θ as:

$$\theta(y) = 2 \arctan\left(\mathrm{e}^{\frac{y}{\Delta}}\right) - \frac{\pi}{2} \tag{2}$$

where Δ is the domain wall width and is equal to $\sqrt{\frac{A}{K_u}}$. The total energy taking into account both exchange and anisotropy terms hence writes:

$$E = \int_{-\infty}^{+\infty} \left[K \cos^2(\theta) + A \left(\frac{\partial \theta}{\partial y}\right)^2 \right] = 4\sqrt{AK_u} = \sigma \tag{3}$$

In the above expression, the domain wall energy is called σ and is directly related to the exchange and anisotropy constants.

1.3 Total energy

As presented in equation 3, the total energy contains the magnetic exchange and the anisotropy that are both inherent to the formation of the domain walls (E_{DW}), but also

the Zeeman energy originating from the applied field (E_{Zeeman}) as well as the magnetostatic energy (E_{mag}, from the stray field). The latter term reads:

$$E_{\text{mag}} = \frac{\mu_0 M_S^2}{2} d \left\{ m^2 + \frac{4p}{\pi^3} \sum_{n=1}^{+\infty} \frac{1}{n^3} \sin^2 \left[\frac{\pi n (1+m)}{2} \right] \left[1 - \mathrm{e}^{\frac{-2\pi n}{p}} \right] \right\} \tag{4}$$

where M_S is the saturation magnetization, $p = (W1 + W2)/d$ is the reduced period of the domain walls with $W1$ and $W2$ the average width of the oppositely oriented magnetized domains. Overall, $m = (W1 - W2)/(W1 + W2)$ denotes the reduced magnetization which thus takes into account both directions of magnetization. The total energy ε can therefore be written in units of $\mu_0 M_S^2 d/2$ as:

$$\varepsilon = \underbrace{4 \left(\frac{\lambda_c}{p} \right)}_{E_{\text{DW}}} \overbrace{-2hm}^{E_{\text{Zeeman}}} + \underbrace{m^2 + \frac{4p}{\pi^3} \sum_{n=1}^{+\infty} \frac{1}{n^3} \left[\frac{\pi n (1+m)}{2} \right] \left[1 - \mathrm{e}^{\frac{-2\pi n}{p}} \right]}_{E_{\text{mag}}} \tag{5}$$

where $\lambda_c = \sigma/(\mu_0 M_S^2 d)$ is defined as the characteristic reduced length, and $h = H/M_S$. As shown in the above equation 5, the total energy depends on the domain walls period. This energy minimizes to zero at equilibrium. Therefore, a measure of the period with an experimental apparatus such as the Kerr microscope can give great insight on the exchange and anisotropy constants. At equilibrium, the first derivative of the total energy ε with respect to the reduced period p is zero and reads:

$$\frac{\partial \varepsilon}{\partial p} = -4 \left(\frac{\lambda_c}{p^2} \right) + \frac{4}{\pi^3} \sum_{n=1}^{+\infty} \frac{1}{n^3} \sin^2 \left(\frac{\pi n}{2} \right) \left[1 - \mathrm{e}^{\frac{-2\pi n}{p}} - p \, \mathrm{e}^{\frac{-2\pi n}{p}} \left(\frac{2\pi n}{p^2} \right) \right] = 0 \tag{6}$$

Equation 6 enables us to write then the reduced length as follows:

$$\lambda_c(p) = \frac{\sigma(p)}{\mu_0 M_S^2 d} = \frac{p^2}{\pi^3} \sum_{n=1}^{+\infty} \frac{1}{n^3} \sin^2 \left(\frac{\pi n}{2} \right) \left[1 - \left(1 + \frac{2\pi n}{p} \right) \mathrm{e}^{-\frac{2\pi n}{p}} \right] \tag{7}$$

This sum can be computed thanks to computer calculations but requires accurate measurement of the domain walls period thanks to the use of microscopy able to observe magneto-optic phenomena.

1.4 Faraday effect

Magneto-optic effects originate from the interactions of a magnetic material and a propagating electromagnetic wave. The study of the altered radiation gives therefore great insight to the magnetic properties of the probed material. In 1845, Michael Faraday discovered that the direction of polarization of light passing through a magnetic material was changed by a certain angle of rotation, proportional to the amount of probed material.

In general, light as an electromagnetic wave of angular frequency ω can be described as a propagative plane waves and the optical properties of a material can be described by the dielectric permittivity tensor of rank two $[\varepsilon(\omega)]$. From the Maxwell equations that relate the transverse electric and magnetic field expressed as propagating waves $\mathbf{E}$ and $\mathbf{H}$ and using the expression of the electric displacement $\mathbf{D} = \varepsilon_0 [\varepsilon(\omega)] \mathbf{E}$, it follows:

$$N^2\mathbf{E} = [\varepsilon(\omega)]\,\mathbf{E} \tag{8}$$

where $N = n + i\kappa$ denotes the complex refractive index of the probed material, n standing for the phase speed and κ indicating the amount of absorption (damping) of the propagative electromagnetic wave. The dielectric permittivity of a cubic ferrimagnetic crystal uniformly magnetized along the z-direction below its critical temperature T_C differs from identity and shows components depending on the magnetization and reads:

$$[\epsilon(\omega)] = \begin{bmatrix} \epsilon_{\mathrm{xx}} & \epsilon_{\mathrm{xy}}(M) & 0 \\ -\epsilon_{\mathrm{xy}}(M) & \epsilon_{\mathrm{xx}} & 0 \\ 0 & 0 & \epsilon_{\mathrm{zz}} \end{bmatrix} \tag{9}$$

Solving equation 8 thanks to the above expression of the dielectric tensor gives the following solutions for the two normal modes of propagation of light:

$$N_{\pm}^2 = \varepsilon_{xx} \pm \varepsilon_{xy}(M) \tag{10}$$

The distinct solutions refer to the two normal modes of propagation of light in that case, σ_+ and σ_-, the two circular either left or right polarization. In the case of linearly polarized light, the propagating electric field is composed of evenly distributed σ_+ and σ_- polarization components, forming oscillations in the so-called polarization plane, which contains the wavevector $\mathbf{k}$. Such plane wave is modulated by the factor e^{ikz} where $k = \omega N/c$. Therefore, there is a phase shift between the two normal modes according to the different refractive indices for σ_+ and σ_- polarization. This shift is observed as a rotation of the polarization plane which is the so-called Faraday rotation, of angle:

$$\Theta_F = \frac{\omega}{2c}(n_+ - n_-) \tag{11}$$

Therefore, the rotation of the plane of polarization of the linearly polarized field is a measure of the optical quantities and hence gives insight to the change of magnetization as emphasized by the off-diagonal terms of the dielectric tensor in equation 9.

2 Experimental aspects

2.1 Kerr microscope set-up

The magnetic domains can be observed thanks to the Faraday effect and with the use of a so-called Kerr microscope. The sample under study is a ferrimagnetic layer of $GdPrBi_3(FeAl)_5O_{12}$ of thickness $d = 6$ μm which behaves very much like a ferromagnet, under its critical Curie temperature of about 559 K which is well above the ambient temperature, hence compatible with the observation of magnetic domains for this experiment. It has a saturation magnetization of $M_S = 11.14$ kA/m and a uniaxial anisotropy of constant $K_u = 3.7\ 10^3$ J/m^3. Its magnetization is perpendicular to the plane of the sample. The sample is held on a mirror plane, which is an important part of the set-up described hereafter.

Figure 1 shows a sketch of the microscope. A bright white lamp is used as a source and light of wavelength $\lambda = 670$ nm is selected by an interference filter and focused onto an aperture by a first lens F_1. The set-up is built according to the Köhler illumination which consists in focusing the image of the aperture on the back focal plane of a microscope

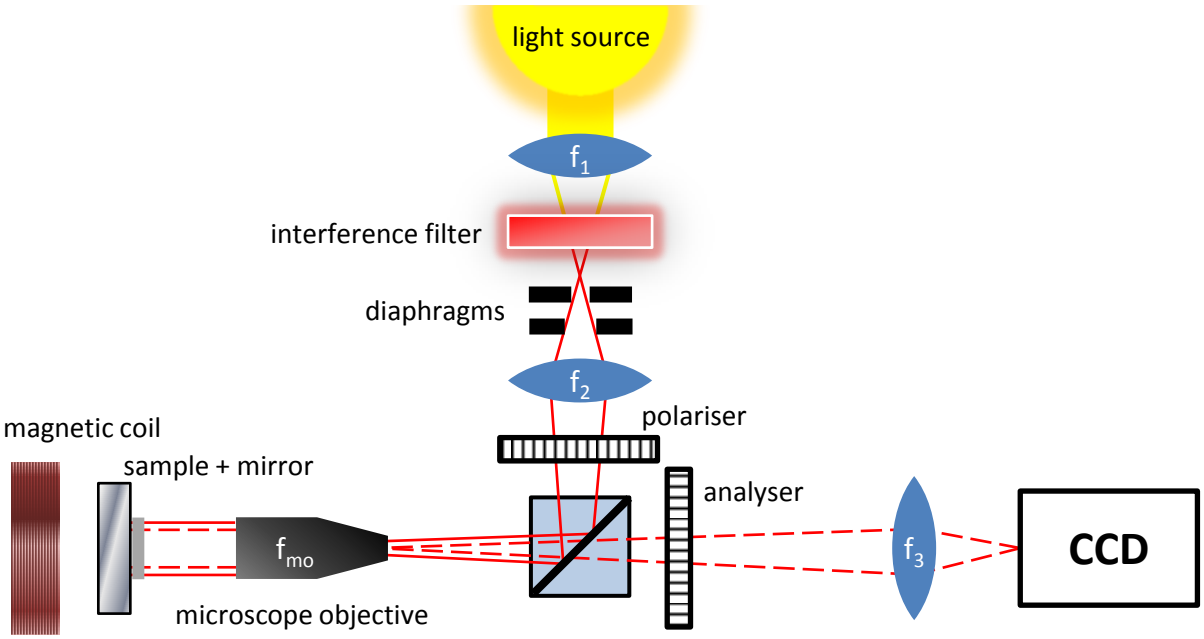

Figure 1: *Illustration of the magneto-optical set-up Kerr microscope. The light source is a white lamp whose red light component ($\lambda \approx 670$ mm) is firstly selected, then focused on an aperture whose image is focused at the back focal plane (BFP) of a microscope objective in order to obtain a homogeneous illumination of the sample which is held on a mirror. A magnetic coil is used to tune the applied magnetic field in the direction parallel or anti-parallel with respect to the incident light. The polarized light is analysed in transmission after going back and forth through the sample thanks to the mirror, before being focused onto a highly sensitive computer driven CCD. The elements of optics are an aperture of millimetre size, and the lenses of focal lengths $f_1 = 50$ mm, $f_2 = 76$ mm, $f_3 = 120$ mm, and $f_{mo} = 9.9$ mm.*

objective in order to shine the sample uniformly: the incident light is polarized linearly thanks to a polariser and is focused by a lens F_2 on a microscope objective of large working distance and numerical aperture $N.A. = 0.4$ which shines the sample homogeneously. Light goes through the probed material and is reflected by the mirror holder on which the latter is glued. Hence light passes twice the sample, which provides a rotation of polarization of angle $2 \cdot \Theta_F$ thanks to the time reversal breaking of the Faraday rotation, enhancing the polarization changes of light going through different magnetic domains. Light is finally analysed and focused by a lens F_3 onto a CCD camera.

The polariser and analyser are the parts of the set-up which allows to experimentally visualize the magnetic domains. Indeed, the linear polarization of light imposed by the polariser is changed thanks to the Faraday rotation and this change can be resolved by aligning the analyser in such a way that the components of light whose polarization have not been affected are filtered out. The observed contrast would therefore be related to the various domains. And in the case of a binary magnetization perpendicular to the plane of the sample, either up or down, the two types of domains can be observed knowing the rotation angle and aligning properly the analyser. Moreover, at fixed position of the analyser, the intensity of light that is not cut out decreases with decreasing rotation angle, i.e. with decreasing magnetization. This is one of the aim of this work, since we use a magnetic coil to tune the applied magnetic field which induces different magnetization in the sample. But the set-up requires a specific work of calibration which is described in the following.

2.2 Calibration

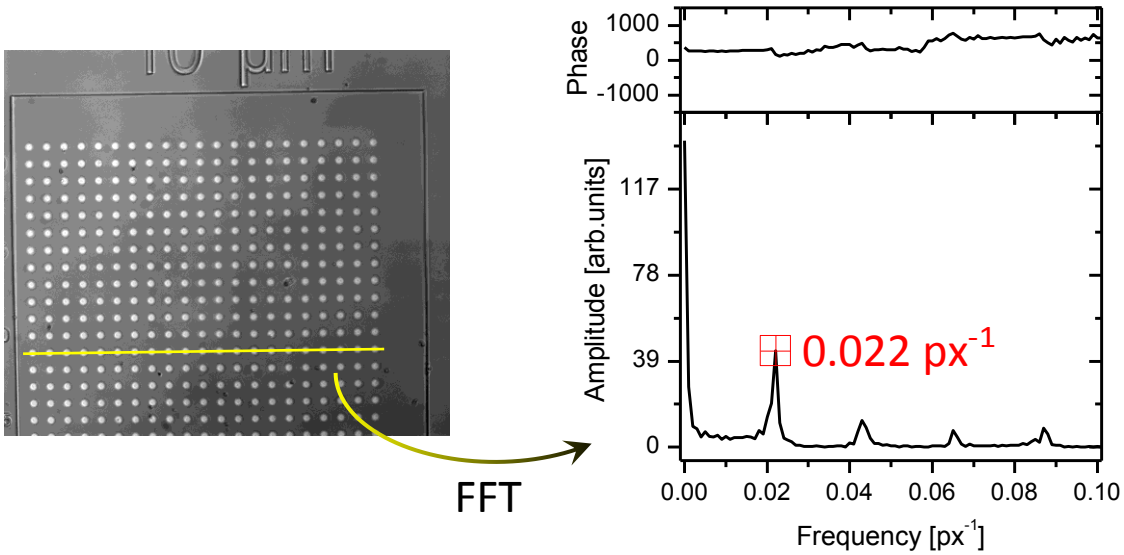

Figure 2: *On the left, a photograph of the calibration plate is depicted where the yellow line corresponds to the direction for which the Fourier transform of the intensity profile is displayed on the right. This allows to obtain an equivalence between pixels and actual distances of the observed samples.*

First of all, we need to know the equivalence between the observed pixels (px) on the image and the actual lengths (μm) on the sample. This is achieve thanks to a patterned plate containing small discs that has been grown by lithography. The discs are separated by a distance of 25 μm. Figure 2 shows the microscope image of the patterned calibration surface and the measurement of the period in terms of pixels. A Fourier transform of the periodic surface is performed and the corresponding period can be accurately determined. The measurement in spatial frequency gives the representation of 1 pixel on an image as 0.55 μm on the sample. Since 1 px is indeed a square of 6.45 μm edge, the measured magnification is therefore:

$$M_{(\text{measured})} = \frac{6.45}{0.55} \approx 11.73$$

This quantity originating from the combination of microscope objective and optical lenses can be calculated thanks to the focal lengths of both the microscope and the lens that focuses onto the CCD camera as follows:

$$M_{(\text{theoretical})} = \frac{f_3}{f_{\text{mo}}} \approx 12.12$$

The little disagreement can be assigned either to misalignment, mispositioning, quality of the optical elements or the measurement of the periods on the calibration plate. Still the magnification can be considered to be of around 12.

A more important quantity can be estimated. The resolution of the optical set-up is determined by the Rayleigh criterion which states that two points separated by a given distance can be resolved if this distance is larger than the distance that separates the principal diffraction maximum of one image to the first minimum of the other. The resolution reads:

$$R = 1.220 \cdot \frac{\lambda}{2 \cdot NA} = 1.220 \cdot \frac{670 \text{ (nm)}}{2 \cdot 0.4} = 1.02 \ \mu\text{m}$$

The optical resolution involves a Bessel function from which originates the factor 1.220. The resolution found corresponds approximately to two pixels on an image (2×0.55 μm). Two pixels for the smallest resolvable actual length unit is not ideal: a point-like object gives a diffraction spot of whose width can not really be appreciated by only two pixels. Three pixels would at least show a higher intensity for the pixel in between two others and the diffraction spot would be better resolved. Hence the resolution depends mostly on the CCD camera. However, one could change the focal length of F_3 in order to increase the resolution, although it would decrease the illumination area.

3 Results and discussion

3.1 Faraday rotation

Before investigating the magnetic domains thanks to the rotation of the plane of polarization of the probing light, we indeed first measure the value of the Faraday angle Θ_F. Human eye is used as a detector for this measurement. At first, we ensure that light is linearly polarised, that is we check that minima of intensity are reached when the polariser and the analyser are perpendicular to each other. Then, we position the sample on its holder but without the mirror behind it, and put the analyser after it on the optical path. Light is therefore polarized, then passes through the material, and finally goes through the analyser.

negative turning angle	negative magn. field	reference	positive magn. field	positive turning angle
$-6°40'$	$271°50'$	$263°20'$	$277°45'$	$+7°45'$
$-4°50'$	$271°15'$	$264°21'$	$276°50'$	$+6°54'$
$-5°50'$	$271°10'$	$264°50'$	$276°15'$	$+6°20'$

Table 1: *Observed values of the Faraday rotation angle that is the deviation of the plane of polarization with respect to the initial (prior to going through the sample) polarization of light, for both positive and negative applied magnetic field, measured by three different operators.*

A saturating magnetic field of approximately ± 100 Oe is applied onto the sample so that it gets fully magnetized along or oppositely to the incident beam. The analyser is then rotated until light visibly reaches a minimum of intensity. This still occurs when the plane of polarization and the zero-angle of the analyser are perpendicular to each other. We then see the deviation with respect to the reference and collect the turning angles for both saturating positive and negative magnetic field, which are summed up in table 1.

The mean rotation angle induced by the out-of-plane magnetization whether in the direction (negative) or opposite (positive) to the direction of propagation of light is respectively $-5°32'$ and $7°00'$. Even though the absolute values differ while they should not, one notes that the rotation angle is really large and eye measurement is well adapted for adjustments and references. More importantly, this large deviation of the plane allows to resolve different magnetization and domains very well in terms of intensity contrast.

3.2 Period of magnetic domains

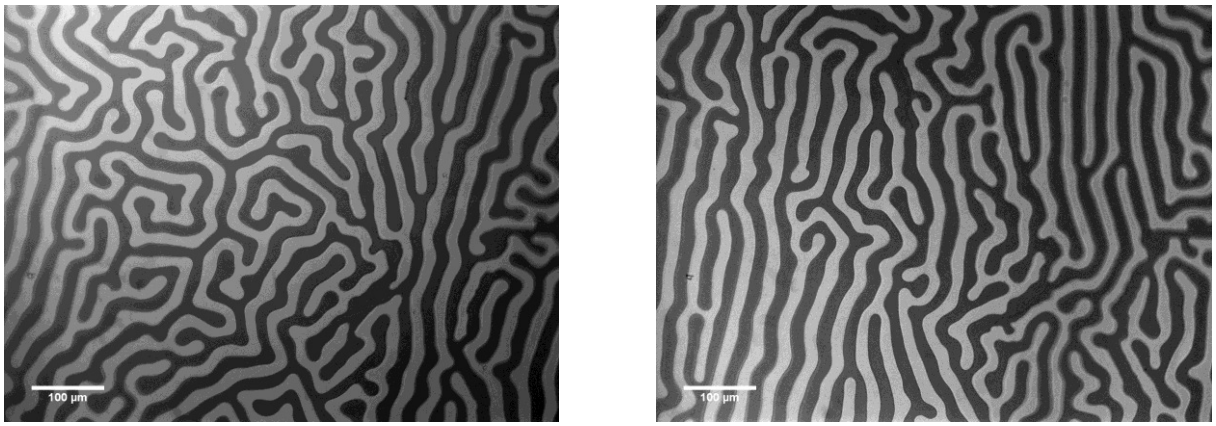

(a) *MO image* **(b)** *MO image*

Figure 3: *Magnetic domains showing different magnetization directions in the material without magnetic. The contrast results in different magnetization which rotates the plane of polarization of the transmitted light which is then filtered. In the case of image 3a, the magnetization is observed without any applied magnetic field whereas in image 3b, a magnetic field was applied in the plane of the sample. The latter case shows more parallel stripes which mostly result in the alignment of the domains with the applied field.*

The magneto-optical images are were obtained in transmission with the probing light passing back and forth through the garnet sample glued on a mirror. The magnetization inducing deviation of polarization is observed by variation of contrast thanks to the selection of specific polarization angle. Figure 3 shows the magnetic domains obtained thanks to the Kerr microscope set-up. Both images present stripes of regular width with varying shapes and orientations. Image 3a shows more rounded shapes and turns, with domain walls rather randomly oriented. This image has been taken without any applied field and result in the remaining magnetization of the ferromagnetic material under study. Next to it, image 3b is characterized by the same type of stripes but a favoured orientation of the domains can be observed. The period of the stripes looks comparable to the one of the other image. The material was subjected to an external applied field directed in the plane of the sample, which caused this preferred orientation of the magnetic domains, with magnetization directed more or less along the applied field.

The period of the stripes was measured for both images as the average of numerous measurements using the program *ImageJ* and a rather handy plug-in. The resulting periods are:

$$P_{(a)} = 30.29 \pm 0.42\ \mu\text{m} \qquad P_{(b)} = 33.67 \pm 1.09\ \mu\text{m}$$

The two measurements show a deviation beyond the standard deviation which can not be solely assigned to the fewer measurements on image 3a (13 versus 40 values for 3b) but also to the fact that they were performed by two distinct operators who inserted different systematic errors. However, the value with the smallest standard deviation (i.e. $P_{(a)}$) is taken as reference for further calculations. As a matter of fact, the period appears in the reduced length in equation 7 and allows to calculate the exchange constant as expressed in σ in equation 3. It comes:

$$A = \frac{(\lambda_c \mu_0 M_S^2 d)^2}{16 K_u} = 16.06 \cdot 10^{-12} \text{ J/m}$$

Literature values[1] for other ferromagnetic materials such as $A(BaFe_{12}O_{19}) = 6 \cdot 10^{-12}$ J/m or $A(SmCo_{15}) = 24 \cdot 10^{-12}$ J/m show relative good agreement with the calculated value for our garnet sample, being in a correct order of magnitude. Knowing the anisotropy constant K_u of our material, one can estimate the domain wall width, such that:

$$\Delta = \sqrt{\frac{A}{K_u}} = 0.208 \ \mu\text{m}$$

This calculated value is well below the actual spatial resolution of the set-up (limited by the CDD camera) which is of around 1 μm. This shows the power of this set-up and set of optical measurements which allow to collect information on structures that are too small to be observed directly. Nevertheless, it is possible to actually see the domain walls and the spatial segregation of magnetization on the sample. Figure 4a shows a magneto-optical image obtained with aligned polariser and analyser, such that both directions of magnetization can pass the analyzer. In other words, the light with the two possible direction of polarization (with negative or positive rotation angle) can pass the analyzer so that only the domain walls with transient magnetization can not pass. Moreover, light at the domains is diffracted and scattered away in such a way that the domain walls appear as low contrast compared to the actual domains. The profile in figure 4b depicts a domain interface is presented and the full width at half maximum depicts the achieved spatial resolution of this optical method. We find a wall of width approximately 2 μm which emphasizes the fact that this quantity shall be calculated whenever the set-up doesn't allow to reach high enough resolution.

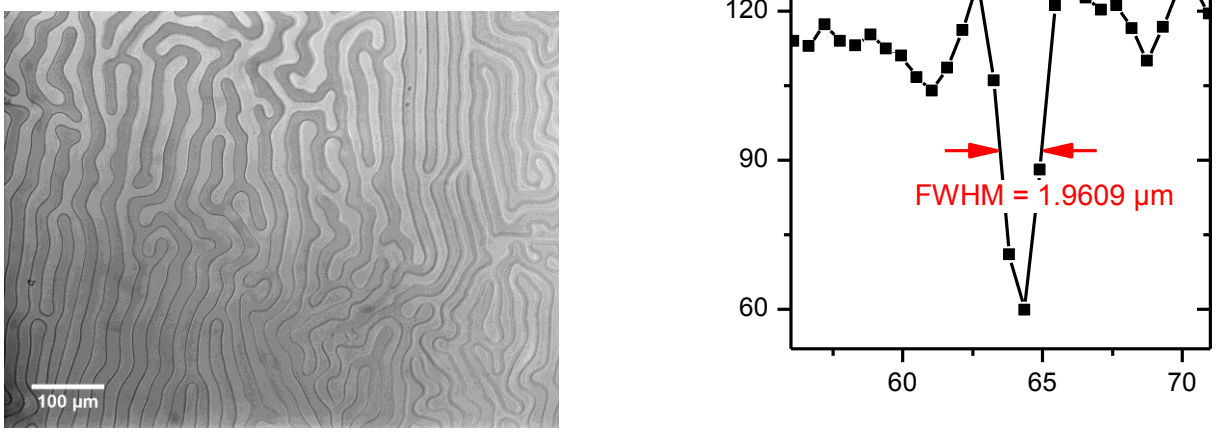

(a) *Magnetic domains* **(b)** *Domain period*

Figure 4: *Magneto-optical image of the domain walls obtained by aligning the polarisers such that both direction of magnetization can be observed. The profile on the right illustrates the intensity at a domain wall.*

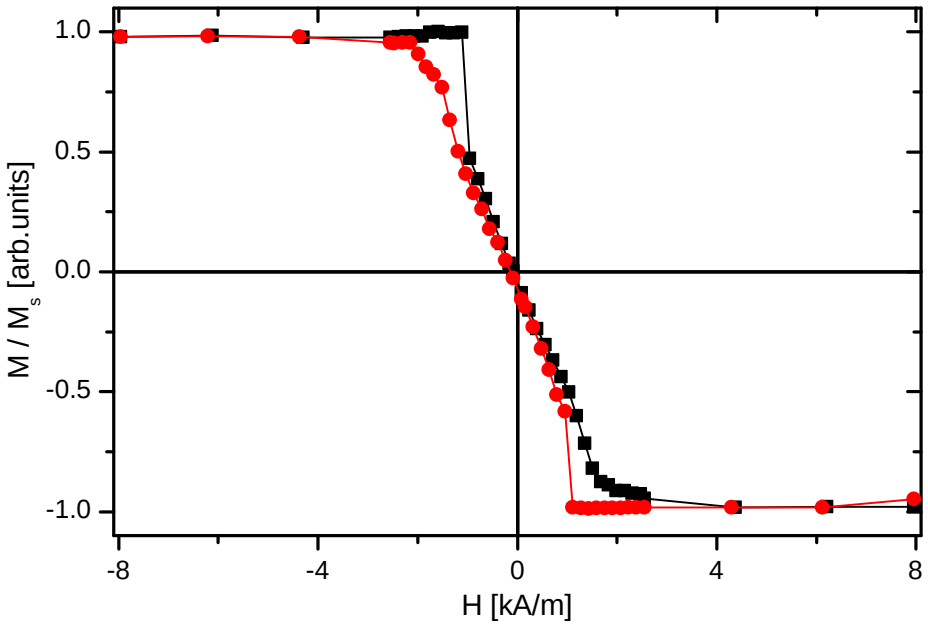

Figure 5: *Profile of normalized magnetization with respect to the applied magnetic field on the garnet sample thanks to magneto-optical measurements, showing a characteristic hysteresis behaviour. The black line was obtained by tuning the magnetic strength from negative to positive values whereas the red line depicts the opposite procedure, tuning the magnetic field from positive maximum to the opposite minimum.*

3.3 Hysteresis cycle

Thanks to the contrast that exhibits the two different magnetization directions in the sample, it is possible to measure qualitatively the magnetization as a function of the applied field, which we tune from around -100 Oe to $+100$ Oe. The experimental procedure is ensured by a LabVIEW program which iterates the value of the applied field within a certain range by adjusting the current in the magnetic coil and which takes a picture of the illuminated sample at each step. Then, the software counts the number of pixels $N_\uparrow$ with intensity $I_\uparrow$ and the amount $N_\downarrow$ with intensity $I_\downarrow$ for upward ($M_\uparrow = M_S$) and downward ($M_\downarrow = -M_S$) magnetization respectively. The average intensity $< I >$ and the average magnetization $< M >$ are therefore linked within the relations:

$$< I > = \frac{N_\uparrow I_\uparrow + N_\downarrow I_\downarrow}{N_\uparrow + N_\downarrow} \qquad < M > = \frac{N_\uparrow M - N_\downarrow M}{N_\uparrow + N_\downarrow} \tag{12}$$

The mean intensity is averaged over the minimum and maximum of intensity, corresponding to the two directions of magnetization. These are two positive quantities. At saturated magnetization inducing a rotation of polarization such that light can pass the analyzer (applied field of around 8 kA/m), the image is rather white (maximum of intensity) and reversely when the sample is fully magnetized such that the rotated polarization is blocked by the analyzer (external field of around -8 kA/m), the image appears rather black (minimum of intensity). We scan the applied field from negative to positive amplitude and reciprocally, aligning the domains more or less in the direction of propagation of light. We assume the magnetization cycle to be symmetric such that the zero of mean magnetization lies between the maximum and the minimum of mean intensity. We can

[1]E. Du Trémolet de Lacheisserie (ed.) Magnétisme 1 - Fondements, EDP Sciences, 2000

therefore display the magnetization with respect to the applied field, taking the mean intensity fitted to ± 1, centered to 0 and normalizing over the saturation magnetization M_S (with the help of equation 12. We obtain the profile depicted in figure 5.

The magnetization shows a symmetric behavior with respect to zero applied field. The black curve corresponds to a scan of applied field from negative to positive amplitude (from left to right) whereas the red line stands for the reversed scan, that is from positive to negative saturating external magnetic field (from right to left). Both curves superimpose at high amplitude of applied field while they do not follow the same path at low value of external field. This is characteristic of a hysteresis cycle where the amount of energy (here magnetic strength H) required to reverse the magnetization is larger than the one which allowed to reach saturation. Starting from a fully magnetized region, say at the maximum in figure 5, the decrease of amplitude of applied magnetic strength (from -8 to 0 kA/m) leads to an abrupt change of magnetization at around -1 kA/m. This corresponds to the apparition of the magnetic domains, at a point where the intrinsic magnetization can no longer handle the stray field. Then domains of opposite magnetization gets smoothly larger and larger and reach saturation at high applied field. This phenomenon can be explained by the total energy presented in equation 5, which shows a competition between the domains energy that depends on the reduced period p (that is to say their occupancy) and the Zeeman energy of the applied field. The domains energy represents a barrier that has to be overcome by the applied magnetic strength, which is observed in the hysteresis cycle.

An analogous result can be observed with a more sophisticated set-up such as a *SQUID*, which is based on the Josephson effect and measures weak magnetic fields and can map the magnetization of the sample. The figure in annex depicts a hysteresis cycle reversed (this is a matter of convention) which shows the same kind of abrupt variations characteristic of hysteresis. It is comparable to figure 5, symmetric on zero field and shows how powerful and accurate results can be obtained with the home-made Kerr microscope.

Conclusion

This experimental work based on the magneto-optic Faraday rotation effect investigated thanks to a Kerr microscope allowed to observe magnetic domains and their evolution with an external applied field on a ferromagnetic material. The calibration required for the set-up to be well adjusted allowed us to see that we can obtain information on physical quantities that are well below the resolution of the microscope, which really exhibits the power of this set-up together with its comparison with more sophisticated techniques such as SQUID. Magnetic properties of materials are more and more studied and Kerr microscopy represents a tool well adapted for preliminary investigations.